Chemical Physics Letters 686 (2017) 218–222

Contents lists available at ScienceDirect

Chemical Physics Letters

journal homepage: www.elsevier.com/locate/cplett

Editor's choice

# Revisiting the photophysics of 9-fluorenone: Ultrafast time-resolved fluorescence and theoretical studies

Chih-Wei Chang [b,*], Theis I. Sølling [a,*], Eric Wei-Guang Diau [c,*]

[a] Department of Chemistry, University of Copenhagen, Copenhagen, Denmark
[b] Department of Chemistry, National Changhua University of Education, Taiwan
[c] Department of Applied Chemistry and Institute of Molecular Science, National Chiao Tung University, Taiwan

ARTICLE INFO

*Article history:*
Received 28 May 2017
In final form 17 July 2017
Available online 21 July 2017

*Keywords:*
Fluorenone
Time-resolved mass spectroscopy
Time-resolved fluorescence spectroscopy
Intersystem crossing

ABSTRACT

Ultrafast intersystem crossing dynamics of fluorenone in gas and condensed phases were investigated by time-resolved mass spectrometry and fluorescence up-conversion spectroscopy. The former shows the ultrafast Franck-Condon relaxation and the internal conversion dynamics of isolated fluorenone in the gas phase. The latter reveals that the vibrational relaxation time is 2.2 ps and a 110 ps fluorescence lifetime of fluorenone in hexane. The fluorescence lifetime in acetonitrile and dimethylsulfoxide is 16 ns and 15.1 ns, respectively. The potential energy surface along the C=O out of plane bending motion shows that this coordinate is important for ISC in both polar and non-polar solvents.



## 1. Introduction

Understanding the factors that affect the deactivation rate of an excited molecule is key to studies of photoinduced processes. The information is important not only to challenge well established theories, but also when it comes to the design of novel compounds with specifically desired optical properties. It is no surprise that the photophysical properties of a particular chromophore are affected by multiple parameters, such as the molecular structure, the temperature, the viscosity and polarity of solvent [1].

The photophysics of fluorenone is of particular interest because of the extreme sensitivity to the microenvironment [2–9]. In recent years, fluorenone based polymers have received lots of attention due to its desirable optical properties that can be utilized in the light-emitting diode industry [10]. In nonpolar and polar solvents, the lowest singlet excited ($S_1$) state of fluorenone is due to n-$\pi^*$ and $\pi$-$\pi^*$ transitions, respectively [4,5,11]. In a nonpolar solvent, fluorenone exhibits nearly 100% triplet quantum yield due to the ultrafast intersystem crossing (ISC) processes [8]. The previous model suggested that there are two types of intersystem crossing (ISC) processes involved in the relaxation of the $S_1$ state [5]. The first type is temperature independent, which is due to the El-Sayed type ISC dynamics from $S_1$ to $T_1$ ($\pi$-$\pi^*$) and $T_2$ ($\pi$-$\pi^*$) states. This type of ISC is efficient in nonpolar solvents because of the prevalence of the n-$\pi^*$ nature of the $S_1$ state [5]. For fluorenone in polar solvents, the $\pi$-$\pi^*$ character of the $S_1$ state prohibits ISC through such a mechanism. The second type of ISC is from $S_1$ to $T_3$ (n-$\pi^*$). In nonpolar or moderately polar solvents, ISC from $S_1$ to $T_3$ (n-$\pi^*$) shows a strong temperature dependence, which reflects the endothermic nature of this transition [5]. In a polar solvent, the $T_3$ state is located well above the $S_1$ state; and such kind of ISC is also prohibited. Therefore, the internal conversion from $S_1$ to $S_0$ becomes an important deactivation channel of fluorenone and its dipolar derivatives [5,9]. In a polar protic solvent, both singlet and triplet states of fluorenone are quenched due to the formation of intermolecular hydrogen-bond [12–14]. Although the photophysics of fluorenone in condensed phase has been well documented, only little is known about the photophysics of isolated fluorenone. In 2011, Köhler et al. reported the ultrafast time-resolved mass and photoelectron spectra of fluorenone [15]. The molecule was excited around 264–266 nm (which corresponds to the transition to $S_6$). The excited state fluorenone undergoes an ultrafast Franck-Condon relaxation within 50 fs and relaxes to $S_1$ state within 0.4 ps. The small offset component observed in their study was attributed to the ISC from $S_1$ to triplet states [15].

To gain further inside into the photophysics of fluorenone, we have studied the fluorescence life times on the pico- and femtosecond timescale in polar and nonpolar solvents. As reported, the fluorescence lifetime of fluorenone increases with the increasing of solvent polarity. The experiments shed further light on the solvation dynamics of fluorenone in polar solvents. Although the excited state dynamics of fluorenone has been utilized as the model

* Corresponding authors.
*E-mail addresses:* cwchang@cc.ncue.edu.tw (C.-W. Chang), theis@chem.ku.dk (T.I. Sølling), diau@mail.nctu.edu.tw (E.W.-G. Diau).

http://dx.doi.org/10.1016/j.cplett.2017.07.039
0009-2614/

system for singlet and triplet ISC processes for many years, it is surprising that the detailed theoretical studies pertaining to the excited state potential surface (PES) has not been reported yet. In this study, the PES is explored along the C=O out of plane bending coordinate. The result suggests that the C=O out of plane bending motion is important for the ISC dynamics of fluorenone in nonpolar and polar solvents. This seems to even further enhance the El Sayed behavior of the system in a manner that is very similar to what we have recently reported for benzene, toluene and xylene [16]. The information we provide is important for understanding the excited-state dynamics of fluorenone, and more discussions will be found in the following paragraphs.

## 2. Experimental section

### 2.1. Steady state and time-resolved spectroscopy

The 9-fluoreone (98%) was purchased from Sigma and used without further purification. HPLC grade solvents were used as received. The UV–Vis spectra were measured using Cary 50 UV–Vis spectrophotometer. The experimental setups of the picosecond and femtosecond time-resolved spectrometer were described elsewhere [17]. Briefly, the picosecond time-resolved emission spectra were collected using a time-correlated single-photon counting machine (Fluotime 200, PicoQuant). The sample was excited by a vertical polarized picosecond pulsed-diode laser (LDH 375, PicoQuant) and the relative polarization between the excitation and the emission was selected at magic angle (54.7°) condition. The Femtosecond time-resolved spectra were obtained with fluorescence up-conversion spectroscopy (FOG100, CDP). The excitation source was a mode-locked Ti:sapphire laser (Coherent, Mira 900D). The frequency of the laser output was doubled with a type I β-Barium borate (BBO) crystal, and used for excitation. The instrument response related to the up-conversion was about 220 fs (estimated by the third harmonic signal of laser).

### 2.2. Time-resolved mass spectrometry

The time-resolved mass spectrometry (TRMS) experiments were carried out using a femtosecond pulsed laser system and the Copenhagen molecular beam mass spectrometer, which has been described previously [18]. The laser system consists of a chirped pulse amplifier (Spitfire, Spectra Physics) seeded by a femtosecond oscillator (Tsunami, Spectra Physics). The amplifier delivers 800 nm pulses of 100 fs duration (FWHM) and 1 mJ energy at 1 kHz repetition rate. The output was divided by a 50:50 beam splitter into two parts pumping an OPA (TOPAS-C, Light Conversion) and a higher harmonics generation setup, respectively. The latter setup delivered the 400 nm (second harmonic of the fundamental) pulses used as probe pulses with energy of 8.0 μJ. The 258 nm pump pulses, with energy of 1.0 μJ, were generated by collinear sum frequency mixing of the OPA output (signal) and the 800 nm fundamental following by frequency doubling. The time delay between the pulses was controlled by a motorized translation stage. The stage and the data acquisition were controlled by a Labview routine. The in situ one pump + two probe photon cross correlation between the pulses was estimated to be 140 fs using acetone. In the interaction region a continuous molecular beam was intersected at right angle by the incoming laser pulses. The beam was generated by supersonic expansion of 0.3 bar He carrier gas seeded with sample vapor generated by sublimation of the solid sample. To prevent condensation of sample in the expansion nozzle, it was heated to 100 °C while the temperature of the sample container was lower.

### 2.3. Computational methods

The ab initio calculations were performed using G09W software [19]. The ground state geometries of 9-fluorenone with different C=O out of plane bending angles were optimized at the B3LYP/6-311+G(d) level of theory. The structures were used to calculated the vertical excitation energy using the TDDFT method at the B3LYP/6-311++G(d,p) level of theory.

## 3. Results and discussion

### 3.1. Steady state and time-resolved mass spectrometry studies

Fig. 1 shows the steady state absorption and emission spectra of fluorenone in hexane, acetonitrile (ACN), and methanol (MeOH) solutions. In hexane, the $S_1$ absorption and the emission maxima were found at 380 and 500 nm, respectively. Both the absorption and emission spectra show a bathochromic shift in ACN. The larger Stoke's shift in ACN indicates that fluorenone has a larger dipole moment in the excited state. The dipole moment difference ($\Delta\mu$) between the $S_1$ state and the ground state of fluorenone is about 2.2–2.5 D [13]. In MeOH, the emission of fluorenone is further shifted to 570 nm due to the formation of a hydrogen-bonded complex [13]. To elucidate the excited state dynamics of fluorenone in detail, we performed a time-resolved mass spectrometry experiment for gaseous fluorenone to single out the solvent-solute interactions from the intrinsic chromophore properties. Fig. 2 depicts the temporal evolution of the fluorenone parent ion upon 258 nm excitation [15]. The result is in line with previous studies, in which the initial ultrafast decay is attributed to the Franck-Condon relaxation and the internal conversion to the $S_1$ state, while the offset component is due to the intersystem crossing from the $S_1$ to the triplet state [15].

### 3.2. Ultrafast time-resolved fluorescence spectroscopy

To study the relaxation dynamics of excited fluorenone, we have measured a series of femtosecond time-resolved fluorescence transients of fluorenone in nonpolar and polar solvents. Fig. 3 shows the time-resolved transients of fluorenone in hexane. In the nonpolar solvents, the $S_1$ state is $n \rightarrow \pi^*$ in nature [4,11]. In Fig. 3a, the transients were taken at three different excitation

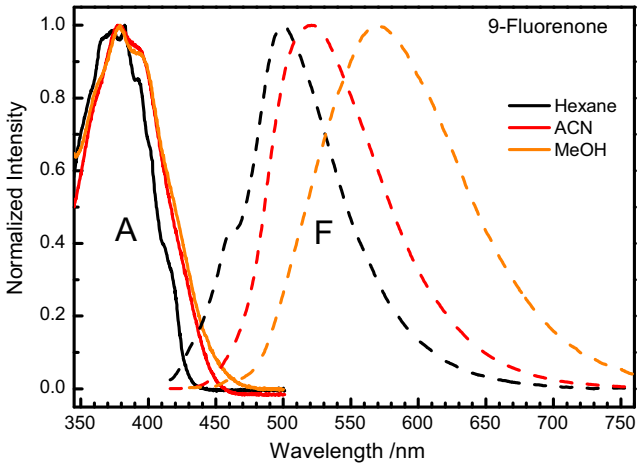


**Fig. 1.** The steady state absorption/emission spectra of fluorenone in hexane, acetonitrile (ACN) and methanol (MeOH) solutions. The excitation wavelengths of the emission spectra were fixed at 400 nm. For clarity, only the longest-wavelength maximum of the absorption spectrum, corresponding to the $S_0 \rightarrow S_1$ transition, is shown.

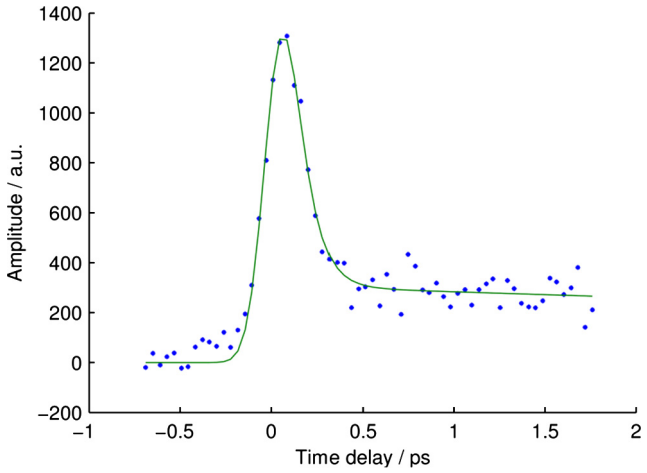


**Fig. 2.** Time-resolved yield of the parent ion of fluorenone as a function of time-delay between the pump (258 nm) and probe (400 nm) pulses in the TRMS experiment.

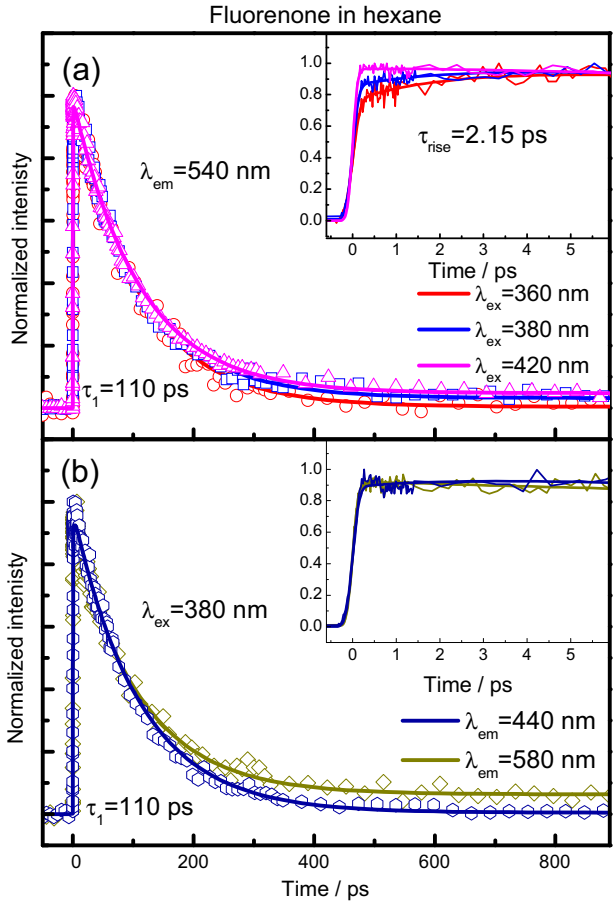


**Fig. 3.** The femtosecond-resolved fluorescence up-conversion results for fluorenone in hexane. The excitation wavelength (a) and the probing wavelength dependence (b) of fluorenone.

wavelengths ($\lambda_{ex}$ = 360, 380 and 420 nm and the emission was fixed at 540 nm. The temporal profiles consist of an ultrafast rise component followed by a decay component ($\tau$ = 110 ps) with a small offset. The rise component can be globally fitted with a time constant of $\tau_{rise}$ = 2.1 ps, and the amplitude of rise component increases with decreasing excitation wavelengths. This energy dependence of the rise suggests that this component is associated with vibrational relaxation of excited state fluorenone. Similar vibrational relaxation dynamics have been reported in a previous transient absorption study, where the vibrational relaxation time of fluorenone in ACN and DMSO was estimated to be 1.4 ps and 2.4 ps, respectively [13]. The 110 ps component is attributed to ISC and our results are in good agreement with the fluorescence lifetime of fluorenone in non-polar solvents as reported in previous studies [4]. We noticed that a small offset appears in the transients when the molecules were excited at the tail of absorption band. In Fig. 3b, the offset component also appears when the fluorescence lifetime was probed at 580 nm, which is at the very end of the emission spectra, i.e., at the bottom of the $S_1$ well. The result could be taken to indicate that the ISC process involves a small energy barrier in which case the offset is a result of the fraction of molecules that do not have enough energy to pass the barrier and that they therefore are trapped at the bottom of $S_1$ state.

Fig. 4 shows the picosecond time-resolved emission spectra of fluorenone in hexane, ACN and DMSO. The 110 ps fluorescence lifetime of fluorenone in hexane is in good agreement with the value obtained from the fluorescence up-conversion studies. In the polar solvents the order of the states are interchanged so that $S_1$ becomes $\pi \rightarrow \pi^*$ in nature just as the lower lying triplet. Thus, in the polar solvents, the spin forbidden ISC between the $S_1$ state and nearby triplet states is not supported by any El-Sayed type effects [4–6,11]. Thus, the resulting fluorescence lifetimes of fluorenone in acetonitrile and DMSO become 16 ns and 15.1 ns, respectively.

### 3.3. Theoretical calculations

The information about the excited state PES along the molecular deformation that we find most likely is involved in the photophysical process of fluorenone is addressed here to shed further light on the fluorescence quenching dynamics. In previous studies, time-dependent density function theory (TDDFT) has been utilized to calculate the single point excitation electronic energy of fluorenone and its hydrogen bonded complexes [14,15,20]. Here, the ground state of fluorenone was optimized at B3LYP/6-311+G(d) level of theory. The structure of fluorenone in ACN was also optimized using the PCM model at the same level of theory. Fluorenone is found to have a planar structure in both cases. The vertical excitation energies were calculated using TDDFT method at B3LYP/6-

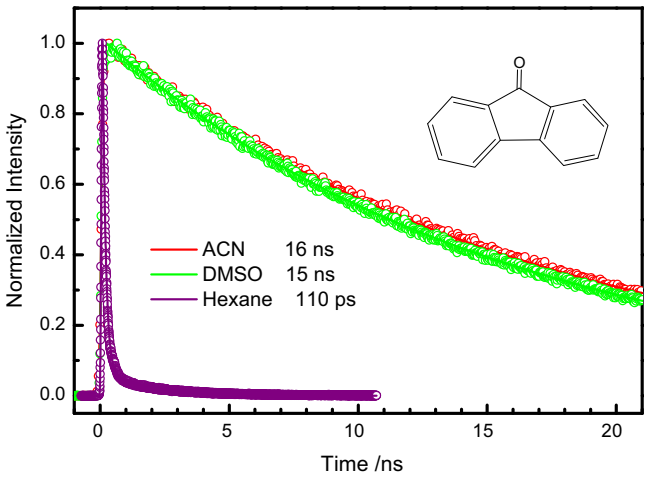


**Fig. 4.** The picosecond-resolved fluorescence transients for fluorenone in acetonitrile and DMSO. The excitation wavelength was fixed at 375 nm and the transient was probed at 520 nm for acetonitrile and DMSO whereas the probe wavelength was 500 nm in the case of hexane.

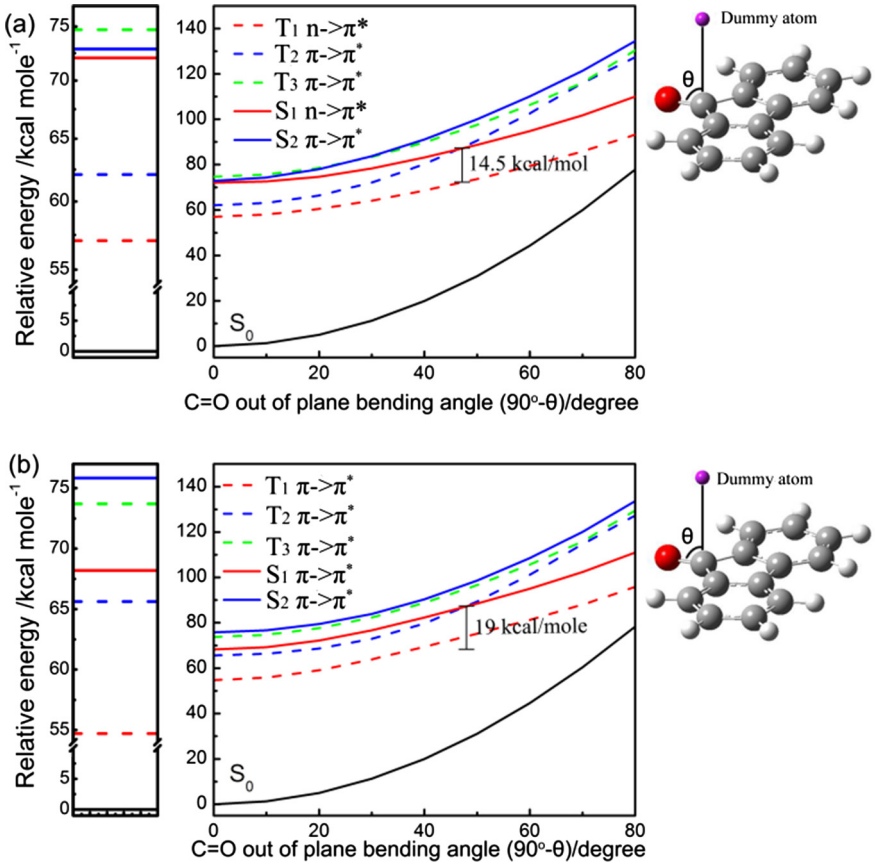


**Fig. 5.** The single point excitation energy and the PES scan along the C=O out of plane bending coordinate of fluorenone (a) in vacuum (b) in acetonitrile. The left panel shows the vertical excitation energy of the planar structure.

311++G(d,p) level, and the results are summarized in Fig. 5. The corresponding energies and oscillator strengths of the lowest six singlet and triplet states are summarized in Table S1 of the supporting information. The related molecular orbitals are depicted in Table S2. The molecular orbital analysis reveals the n → π* and π → π* nature of the $S_1$ state of fluorenone in vacuum and ACN, respectively. The result is in good agreement with previous experimental observations [4,6,11]. We also calculated the PES along C=O out of plane bending coordinate and the result were summarized in Fig. 5. For clarity, singlet and triplet states were indicated by solid and dash lines, respectively. In the vacuum (Fig. 5a), the $S_1$ state corresponds to a n → π* transition and the two close-lying triplets states ($T_2$ and $T_3$) are π → π* in nature. Because the ISC from the n → π* state to the π → π* state are spin-orbital allowed as per El-Sayeds rule [1], the ISC process will involve at least two different mechanisms. The first mechanism is the ISC between $S_1$ and $T_3$. According to our calculations, ISC through this mechanism needs to cross a barrier of least 3 kcal/mol. The second mechanism is the ISC between $S_1$ and $T_2$ which involves a C=O out of plane bending motion to reach the crossing point between $S_1$ and $T_2$. The energy barrier is ~14.5 kcal/mol. The temperature dependence of the ISC rate of fluorenone has been reported previously and indicates that the energy barrier of ISC in fluorenone in non-polar solvents is ~2–3 kcal/mol [5,6]. Therefore, the first mechanism is most likely the primary mechanism for ISC of fluorenone in non-polar solvents and gas phase. However, for excited-state molecules with enough energy, the ISC that takes place via the C=O out of plane bending coordinate might become important. For fluorenone in acetonitrile, the $S_1$ state is π → π* in nature and the ISC between $S_1$ and nearby triplet states are spin-orbital forbidden. It is foreseen that the ISC rate and the triplet quantum yield of fluorenone in polar solvents will be lower compared to their polar counterparts [5,6]. The triplet state quantum yield of fluorenone is 0.46 in ACN [5]. The result suggests the ISC and fluorescence rates in ACN are comparable. The partially (El-Sayed) allowed ISC might occur through two different pathways. The first pathway is the ISC between $S_1$ and $T_3$. Although $T_3$ state is a π → π* transition, the one electron excitation coefficient suggests some n → π* contribution (Table S1) which makes the ISC from $S_1$ to $T_3$ partially spin-orbital allowed. The second pathway is the ISC between $S_1$ and $T_2$. According to our PES scan, the C=O out of plane bending motion will lead to a crossing point between these two states. Although the $T_2$ state is purely π → π* state in planar structure, this state will become a mixed π → π*/n → π* transition along the C=O out of plane bending coordinate. The barrier for this process is ~19 kcal/mol (Fig. 5b), therefore it only occurs for molecules with large excess energy.

## 4. Conclusion

The excited state dynamics of fluorenone in gas phase and polar/nonpolar solvents were investigated in this study. Upon excitation, the time-resolved mass spectroscopy of isolated fluorenone reveals the ultrafast Franck-Condon relaxation and internal-conversion to the $S_1$ state. The offset component found in time-resolved mass spectroscopy is due to the ISC from the $S_1$ to other triplet states. Meanwhile, the ultrafast time-resolved fluorescence studies reveal the 2.2 ps vibration relaxation time and the 110 ps fluorescence lifetime of fluorenone in hexane. The sub-

nanosecond fluorescence lifetime and near 100% triplet quantum yield of fluorenone in the non-polar solvent is due to the efficient ISC processes in $S_1$ state. To address the photophysics of fluorenone in detail, we have performed the PES calculation along the C=O out of plane bending coordinate in vacuum and acetonitrile. The computational results suggest that the C=O out of plane bending reaction coordinate is also a possible ISC reaction coordinate for fluorenone in nonpolar and polar solvents. For fluorenone in nonpolar solvents, the $S_1$ state is a $n \rightarrow \pi^*$ transition. The ISC between $S_1$ and nearby $T_3(\pi \rightarrow \pi^*)$ is the primary deactivation process of the excited fluorenone. However, the crossing point between $S_1$ and $T_2$ might be involved in the ISC of fluorenone when the molecule has enough energy. For fluorenone in ACN, the $S_1$ state becomes a $\pi \rightarrow \pi^*$ transition. Since the nearby triplet states are both $\pi \rightarrow \pi^*$ in nature, the ISC rates between these states are very low because they involve transitions between orbitals with the same angular momentum. However, the moderate triplet state quantum yield for fluorenone in ACN indicates that the ISC in ACN is not totally prohibited and the rate is still fast enough to compete with the fluorescence decay. The partially allowed ISC is due to some $n \rightarrow \pi^*$ nature of the $T_3$ state, therefore the ISC between $S_1$ and $T_3$ becomes possible. In ACN, the crossing point found along the C=O out of plane bending coordinate might be also an important channel for the ISC of highly excited fluorenone. In summary, we have reported a detailed study of the photophysics of fluorenone based on the ultrafast time-resolved spectroscopy and theoretical calculations. The information we have provided reveals the possibility of a novel reaction coordinate for fluorenone in nonpolar and polar solvents, which is important for understanding the photophysics of this long-standing model compound.

## Acknowledgements

We thank Dr. Tsai-Te Wang and Dr. Rasmus Y. Borgaard for their assistance on experiments.

## Appendix A. Supplementary material

Supplementary data associated with this article can be found, in the online version, at http://dx.doi.org/10.1016/j.cplett.2017.07.039.

## References

[1] N.J. Turro, V. Ramamurthy, J.C. Scaiano, Principles of Molecular Photochemistry, University Science Books, 2009.
[2] K. Yoshihara, D.R. Kearns, J. Chem. Phys. 45 (1966) 1991–1999.
[3] T. Kobayashi, S. Nagakura, Chem. Phys. Lett. 43 (1976) 429–434.
[4] L.J. Andrews, A. Deroulede, H. Linschitz, J. Phys. Chem. 82 (1978) 2304–2309.
[5] L. Biczók, T. Bérces, J. Phys. Chem. 92 (1988) 3842–3845.
[6] L. Biczók, T. Bérces, F. Márta, J. Phys. Chem. 97 (1993) 8895–8899.
[7] L. Biczók, T. Bérces, H. Inoue, J. Phys. Chem. A 103 (1999) 3837–3842.
[8] M.K. Nayak, S.K. Dogra, J. Photochem. Photobiol., A 169 (2005) 299–307.
[9] L. Biczók, T. Bérces, T. Yatsuhashi, H. Tachibana, H. Inoue, Phys. Chem. Chem. Phys. 3 (2001) 980–985.
[10] W. Porzio, S. Destri, M. Pasini, U. Giovanella, M. Ragazzi, G. Scavia, D. Kotowski, G. Zotti, B. Vercelli, New J. Chem. 34 (2010) 1961–1973.
[11] L.A. Estrada, J.E. Yarnell, D.C. Neckers, J. Phys. Chem. A 115 (2011) 6366–6375.
[12] L. Biczók, T. Bérces, H. Linschitz, J. Am. Chem. Soc. 119 (1997) 11071–11077.
[13] V. Samant, A.K. Singh, G. Ramakrishna, H.N. Ghosh, T.K. Ghanty, D.K. Palit, J. Phys. Chem. A 109 (2005) 8693–8704.
[14] G.J. Zhao, K.L. Han, J. Phys. Chem. A 111 (2007) 9218–9223.
[15] J. Köhler, P. Hemberger, I. Fischer, G. Piani, L. Poisson, J. Phys. Chem. A 115 (2011) 14249–14253.
[16] A.B. Stephansen, T.I. Sølling, Struct. Dyn. 4 (2017) 044008.
[17] C.W. Chang, C.J. Bhongale, C.S. Lee, W.K. Huang, C.S. Hsu, E.W.G. Diau, J. Phys. Chem. C 116 (2012) 15146–15154.
[18] N. Rusteika, K.B. Møller, T.I. Sølling, Chem. Phys. Lett. 461 (2011) 193–197.
[19] M.J. Frisch, G.W. Trucks, H.B. Schlegel, G.E. Scuseria, M.A. Robb, J.R. Cheeseman, G. Scalmani, V. Barone, B. Mennucci, G.A. Petersson, H. Nakatsuji, M. Caricato, X. Li, H.P. Hratchian, A.F. Izmaylov, J. Bloino, G. Zheng, J.L. Sonnenberg, M. Hada, M. Ehara, K. Toyota, R. Fukuda, J. Hasegawa, M. Ishida, T. Nakajima, Y. Honda, O. Kitao, H. Nakai, T. Vreven, J. Montgomery, J. A., J.E. Peralta, F. Ogliaro, M. Bearpark, J.J. Heyd, E. Brothers, K.N. Kudin, V.N. Staroverov, R. Kobayashi, J. Normand, K. Raghavachari, A. Rendell, J.C. Burant, S.S. Iyengar, J. Tomasi, M. Cossi, N. Rega, J.M. Millam, M. Klene, J.E. Knox, J.B. Cross, V. Bakken, C. Adamo, J. Jaramillo, R. Gomperts, R.E. Stratmann, O. Yazyev, A.J. Austin, R. Cammi, C. Pomelli, J.W. Ochterski, R.L. Martin, K. Morokuma, V.G. Zakrzewski, G.A. Voth, P. Salvador, J.J. Dannenberg, S. Dapprich, A.D. Daniels, Ö. Farkas, J.B. Foresman, J.V. Ortiz, J. Cioslowski, D.J. Fox, Gaussian, Inc., Gaussian 09 Revision A.02 edn., 2009, vol. Gaussian 09 Revision A.02.
[20] Y. Liu, J. Ding, R. Liu, D. Shi, J. Sun, J. Comput. Chem. 30 (2009) 2723–2727.